Environ. Sci. Technol. **1998**, *32,* 719−725

Structural Characterization of a Fulvic Acid and a Humic Acid Using Solid-State Ramp-CP-MAS ^{13}C Nuclear Magnetic Resonance

ROBERT L. COOK AND
COOPER H. LANGFORD*
Department of Chemistry, University of Calgary, 2500 University Drive NW, Calgary, Alberta, Canada T2N 1N4

This study uses the analysis of ^{13}C nuclear magnetic resonance (NMR) spectra and NMR relaxation parameters to study the structure and functional group distribution of a fulvic acid and a humic acid. The spectra and relaxation parameters are obtained with a new cross polarization magic angle spinning (CP-MAS) ^{13}C NMR technique that gives qualitatively and quantitatively accurate results at higher fields. The analysis of the spectra and relaxation parameters indicates that carbohydrate moieties play a major structural role in the fulvic acid studied and contain the major chemical functionality. This analysis also suggested that the majority of the weakly acid protons may be aliphatic/carbohydrate -OH and not phenolic alcohols, as assigned earlier. Models for the fulvic acid and the humic acid are proposed based on spectra and relaxation parameters obtained. The fulvic acid model consists of three units: (i) large relatively immobile units that are mainly aliphatic in nature and largely unfunctionalized; (ii) relatively unfunctionalized more mobile units that are mainly aromatic in nature; and (iii) and more mobile functionalized units that are mainly carbohydrate in nature. The humic acid model consists of one major immobile unit associated with slightly more mobile functionalized units that are mainly aromatic in nature.

Introduction

Humic materials are found in our soils and waters, and they play a major role in both media. Yet, they are among the least understood and characterized components of soil and water. This is not from lack of effort, but mainly the complexity of these materials. Humic materials can be described as complex polydisperse polymeric mixtures, whose properties echo their structural diversity as well as their state of aggregation, conformation, and surface charge distribution. Thus, knowledge of individual molecular components could not alone reveal properties emerging via interaction. Moreover, limited success in trying to fractionate humic materials into individual molecular components leads to the conclusion that the study of humic materials must use methods that are capable of interrogating intact samples. Also, a method that scans one or more monitoring variables is most successful. Synchronous fluorescence provides an example (*3*).

The use of ^{13}C nuclear magnetic resonance (NMR) spectroscopy in the study of humic materials has proven to be a very successful and powerful approach, as it allows for the interrogation of intact samples (*4, 5*). The most popular ^{13}C NMR technique for the study of humic materials and coals is the combination of cross polarization (CP) and magic angle spinning (MAS) on solids. The advantages of the solid state over the liquid state is that there is no concentration limit and no solubility concerns, the solid state is more stable over time than solutions, and there is less sample handling involved. The CP-MAS technique also has the advantage of giving more signal in less accumulation time. There are two factors leading to this increase: first, the gyromagnetic ratio of ^{1}H is four times that of ^{13}C; second, and even more important, the spin−lattice relaxation of protons and not the spin-lattice relaxation of the carbons (^{13}C) dictates the speed with which scans can be obtained. Since the relaxation rate of protons is 2−3 orders of magnitude faster than that of ^{13}C, many more scans can be obtained via the CP-MAS technique in a fixed amount of time. It is now possible to obtain good relaxation parameters for humic materials within a reasonable spectral aquisition time (2−4 days).

However, there have been questions as to the qualitative reliability of the CP-MAS technique (*3*, *6*−*11*). These questions come about because the CP-MAS technique can bias non-protonated carbons. Recently a new CP-MAS procedure for the study of humic materials has given spectra in excellent agreement with the liquid state spectra for Laurentian fulvic acid (*1*, *2*). However, this new CP-MAS procedure has only yielded spectra in good agreement with the liquid spectra for Laurentian humic acid. There are many possible reasons for this, one is that there are more stable radicals on the aromatic rings (as discussed later in this paper). Another is the loss of organic matter during filtration (needed to eliminate line broadening in liquid samples), and the liquid state ^{13}C NMR spectrum may not be an accurate qualitative and quantitative representation of the carbon distribution of Laurentian humic acid (*2*). Regardless, the new CP-MAS procedure produces spectra in much better agreement with the liquid-state spectra than those obtained via the standard CP-MAS method. This new procedure uses ramped amplitude cross polarization (Ramp-CP), rapid sample spinning, and a relatively long contact time [when compared to previously published contact times (*5*, *12*)] on a high field instrument. This study reports chemical shift spectra along with relaxation parameters that elucidate structural and functional group distributions in a fulvic acid and a humic acid using Ramp-CP-MAS ^{13}C NMR.

Pulse Sequences

Ramp-CP. Ramp-CP is a relatively novel approach to cross polarization first introduced by Smith and co-workers (*13*). The Ramp-CP method of cross polarization can be placed in a family of techniques known as variable amplitude cross polarization (VACP). The Ramp-CP pulse sequence is the same as the classic CP [single amplitude cross polarization (SACP)] pulse sequence except one of the spin-lock conditions is varied continuously (Figure 1a); in this study, the proton spin-lock condition. Ramp-CP covers a range of cross polarization frequencies centered on the Hartman−Hahn match (HH) frequency. It has been shown that a ramp centered on the −1 side band gives the best results (*13*). The scan range (although it can be made smaller or larger, see ref 13 for further discussion) of the ramp is set equal to the spinning rate. Ramp-CP overcomes the motional modulation of the CH coupling caused by spinning the sample at a high rate, by changing one of the spin-lock conditions to compensate for the high spinning speed (*1*). It also allows

* Corresponding author e-mail: chlangfo@acs.ucalgary.ca.

S0013-936X(97)00488-4 CCC: $15.00
Published on Web 01/30/1998

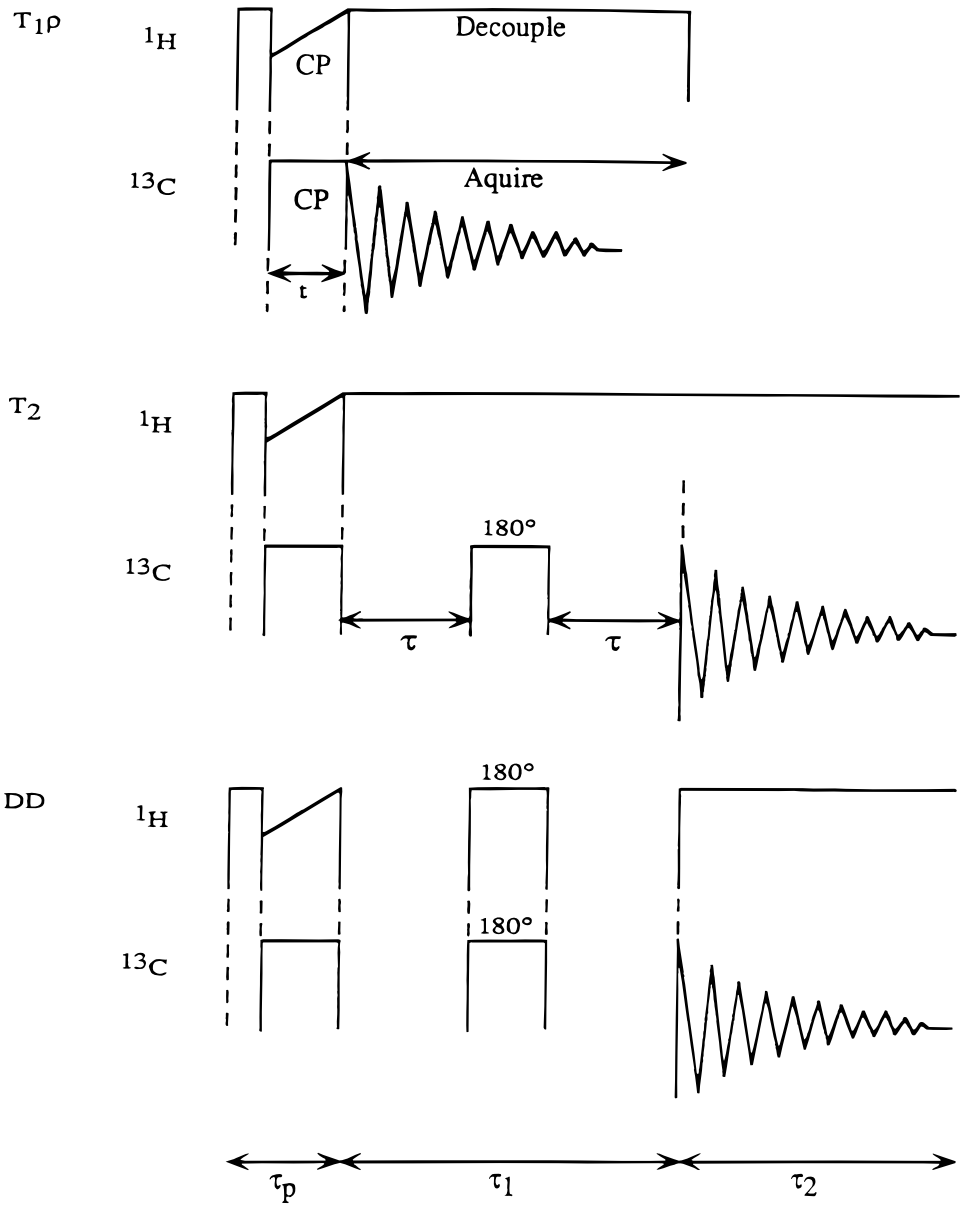

FIGURE 1. Pulse sequences used in this study: (a) the Ramp-CP pulse sequence, see text for details. (b) The pulse sequence for obtaining T_2^{13}C relaxation times, see text for details. (c) The two-dimensional dipolar dephasing pulse sequence, see text for details.

for more than just one HH condition to be matched for samples that are mixtures (*1*, *2*). These advantages of Ramp-CP in relation to humic materials have been discussed in much greater details in refs 1 and 2. Ramp-CP can replace classical cross polarization in all pulse sequences without altering the overall result of the pulse sequence.

Chemical Shift Spectra. The chemical shift spectra were obtained using the pulse sequence shown in Figure 1a. This is the classic cross polarization pulse sequence that has been modified to incorporate ramping the ^{1}H spin-lock condition.

Proton Rotating Frame Spin−Lattice Relaxation Time, $T_{1\rho}$(^{1}H). There are two possible approaches to of measuring $T_{1\rho}$(^{1}H) via CP-MAS ^{13}C NMR. The more frequently used approach is to vary the length of the CP contact. This method is the method used in this study. The alternative approach is to vary the length of the ^{1}H spin-lock condition and only at the end allow for CP with a fixed contact time. This second method overcomes some of the disadvantages of the first method; however, it does have its own disadvatages. Because of this disadvantage, it is almost impossible to apply this method to obtaining $T_{1\rho}$(^{1}H) for humic materials.

The experimental data can be plotted as the natural logarithm of signal intensity versus contact time. Initially the plot rises with a slope equal to the rate of CP (T_{CH}^{-1}), after a certain time the curve falls with a slope equal to $-T_{1\rho}(^1\text{H})^{-1}$. In other words, T_{CH} is determined from the short contact times, and $T_{1\rho}$(^{1}H) is determined from the long contact times. This experiment also gives a way of finding the contact time that is optimal and gives the most liquid-like spectra (if a comparison liquid-state spectrum is available). For a more thorough discussion on $T_{1\rho}$(^{1}H) see refs 5 and 14−16.

Carbon-13 Spin−Spin Relaxation Time, T_2(^{13}C). The preferred method of measuring T_2(^{13}C) in solution is via the Carr−Purcell pulse sequence, in which one uses a 90° pulse followed by a series of equally spaced 180° pulses. This method is inappropriate for solids, since there is a slight cross polarization effect that occurs at each 180° pulse. This is a cumulative effect, and thus after several pulses the relaxation measurement is meaningless (*17*).

However, T_2(^{13}C) can be measured in solids via the Hahn spin-echo method, which can be adapted to CP-MAS (*17*). Figure 1b shows this pulse sequence in the Ramp-CP

modification. After CP, the transverse carbon magnetization is allowed to dephase for a time period, τ. A 180° pulse is applied to the carbons at time τ. After which there is another time delay, τ, during which the fraction of the carbon magnetization, which has decayed due to inhomogeneous interactions, is refocused. Thus, the 180° pulse can be considered as a refocusing pulse. Data acquisition starts at the end of the second τ period. The reduction of the signal from the initial signal reveals the loss of carbon magnetization caused only by the natural T_2 processes. It is important to note that τ must be an integral multiple of the spinning rate, so that it permits an effective time reversal of all inhomogeneous interactions at the 180° pulse. A plot of ln signal intensity versus 2τ gives a slope equal to $T_2(^{13}C)^{-1}$ (*15*).

Two-Dimensional Dipolar Dephasing (DD). A pulse sequence that produces a two-dimensional (2D) spectrum requires three time periods. The first of these periods is the preparation period, τ_p, during this period the spin system is prepared in a coherent non-equilibrium state. During the next time period, known as the evolution period, the system freely evolves under the influence of the Hamiltonian, H^e, which in this case represents dipolar dephasing. The magnitude of the influence of H^e on the spin system is determined by the length of an evolutionary period, τ_1. The τ_1 evolution must be sampled, and in order to do this a series of experiments with a systematic incrementation of τ_1 must be carried out. The minimium number of τ_1 increments is 32. The final time period is the acquisition or detection period, τ_2. Thus, there are two independent time dimensions τ_1 and τ_2 that give a matrix $S(\tau_1, \tau_2)$ that can be transformed via a 2D Fourier transform to give a frequency-domain matrix, $S(\omega_1, \omega_2)$. The 2D transform can be considered as a succession of two 1D Fourier transforms (*18*). The intensity, *S*, is portrayed by a surface in three-dimensional space of the 2D spectrum. The orthogonal axes ω_1 and ω_2 represent the two independent frequency dimensions (*18, 19*).

The pulse sequence shown in Figure 1c will produce a 2D spectrum. In the pulse sequence, the spin system is prepared by cross polarization, via Ramp-CP, during τ_p. The τ_1 evolution in this experiment is a dipolar dephasing evolution, with a 180° refocusing pulse in the middle of τ_1. This 180° refocusing pulse is placed in the pulse sequence to reverse the chemical shift dephasing and leads to a refocusing of the chemical shift dephasing. Care must been taken to ensure that during the 180° refocusing pulse no CP takes place. A normal chemical shift spectrum is obtained from τ_2 after the 2D Fourier transform.

The dipolar dephasing experiment was first introduced by Opella and Frey (*20*). It was then extended by Wilson (*21*) to the pulse sequence seen in Figure 1c, except SACP was used in τ_p. In a dipolar dephasing experiment there is a delay between CP and the acquisition, during which the ^1H and ^{13}C radio frequencies are off. During the delay, the ^{13}C spins, which are strongly coupled to protons via dipole−dipole interactions, are efficiently dephased (hence, the name dipolar dephasing), causing a large loss in the observed ^{13}C signal. The stronger the dipole−dipole interaction, the faster the dephasing. Thus, the weaker the dipole−dipole interaction is, the longer the delay becomes before the ^{13}C signal is lost.

It can be seen that the ω_1 axis of the DD spectrum is a measure of the dipole−dipole interaction strength of different carbons, i.e., the further the signal extends on the ω_1 axis the weaker the dipole−dipole interaction and the ω_1 axis can be used to indicate the functionalization of different structural moieties. It must be noted that, because methyl groups rotate rapidly even in the solid state, the dipole−dipole interactions between the carbons and protons are almost completely destroyed, hence the methyl carbons will also extend out on the ω_1 axis. The diagnostic point is that the further the moiety's signal extends on the ω_1 axis, the more functionalized that moiety is, and the fewer the protons remaining on the carbons.

TABLE 1. NMR Characterization of LFA

	LFA			
chemical shift assignments	chemical shift regions (ppm)	% TOC	$T_{1\rho}{}^1H$ (ms)	$T_2{}^{13}C$ (ms)
ketonic	220−190	8.8	7.3	11.9
carboxyl	190−162	33.8	4.9	13.1
phenolic	162−145	2.2	6.0	22.7
aromatic	145−108	12.0	5.5	11.4
O−C−O	108−96	3.6	3.6	10.4
carbohydrate	96−50	17.8	2.6	12.3
aliphatic	50−0	21.8	2.8	8.0

TABLE 2. NMR Characterization of LHA

	LHA			
chemical shift assignments	chemical shif regions (ppm)	% TOC	$T_{1\rho}{}^1H$ (ms)	$T_2{}^{13}C$ (ms)
ketonic	220−190	6.5	2.4	7.8
carboxyl	190−162	15.7	3.2	8.3
phenolic	162−145	2.8	4.6	9.1
aromatic	145−108	18.7	4.1	7.8
O−C−O	108−96	1.0	3.6	5.1
carbohydrate 1	96−60	11.9	2.3	6.0
carbohydrate 2	60−50	9.1	2.8	5.1
aliphatic	50−0	34.3	3.0	6.9

Experimental Section

Material, Equipment, and Procedure. This study exploits both the Laurentian fulvic acid (LFA) and Laurentian humic acid (LHA) extracted from a forest podzol from the area controlled by Laval University (Quebec, Canada). They were prepared and purified as described in refs 22 and 23. Both LFA and LHA have been extensively characterized, including elemental analysis, acid−base and metal ion titration curves, emission fluorescence, FT-IR, ^1H NMR, and magnetic circular dichroism (*24*−*27*) as well as synchronous and time-resolved fluorescence of the LFA (*3*). The composition of LFA is 45.1% C, 4.1% H, 1.1% N, 49.7% O, <1 ppm Fe, and <1% ash; that of LHA is 51.9% C, 5.5% H, 2.3% N, 39.9% O, 6 ppm Na, and 2 ppm Fe.

All spectra were obtained on a Bruker AMX2-300 spectrometer with a BL4 probe. The rotor was a 4 mm/18 zirconia rotor with a Kel-f cap. All solid-state spectra were obtained at 75.469 MHz, a contact time of 3 ms for LFA, and 2.5 ms for LHA (except for the series of experiments carried out at different contact times, vide infra), a 1 s recycle time, and a sample spinning rate of 8 kHz. The 8 kHz sample spinning rate has been shown to remove chemical shift anisotropy effects for this sample (*1*). A standard contact time experiment (where the contact time is varied) revealed that a contact time of 3 ms for LFA and 2.5 ms for LHA gave spectra that were in good agreement with the liquid spectra, in terms of both qualitative and quantitative sampling of the carbon distribution. This experiment also showed that $T_{1\rho}H >> T_{CH}$, and thus the CP experiment does work on this sample. The 1 s recycle time was found to allow for the complete relaxation of the system, as has been reported by Schnitzer and Preston (*28*).

Data Analysis. The one-dimensional (1D) spectra were processed with the 1D WIN-NMR software package from Bruker, following ref 1. The 2D spectra were processed in a manner very similiar to the 1D spectra, except X-WIN NMR software from Bruker was used.

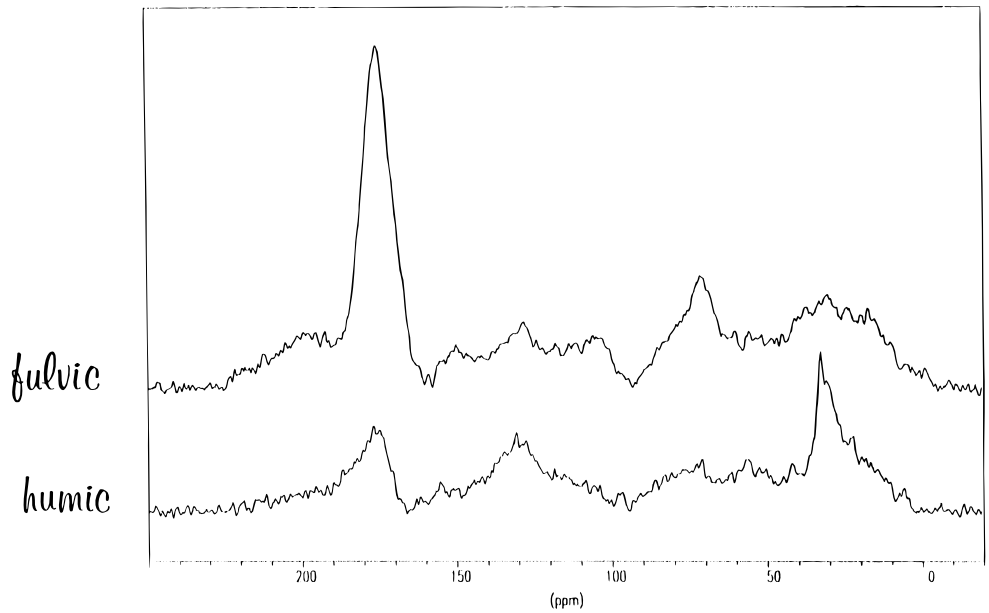

FIGURE 2. Ramp-CP-MAS ^{13}C NMR spectra of LFA (top) and LHA (bottom).

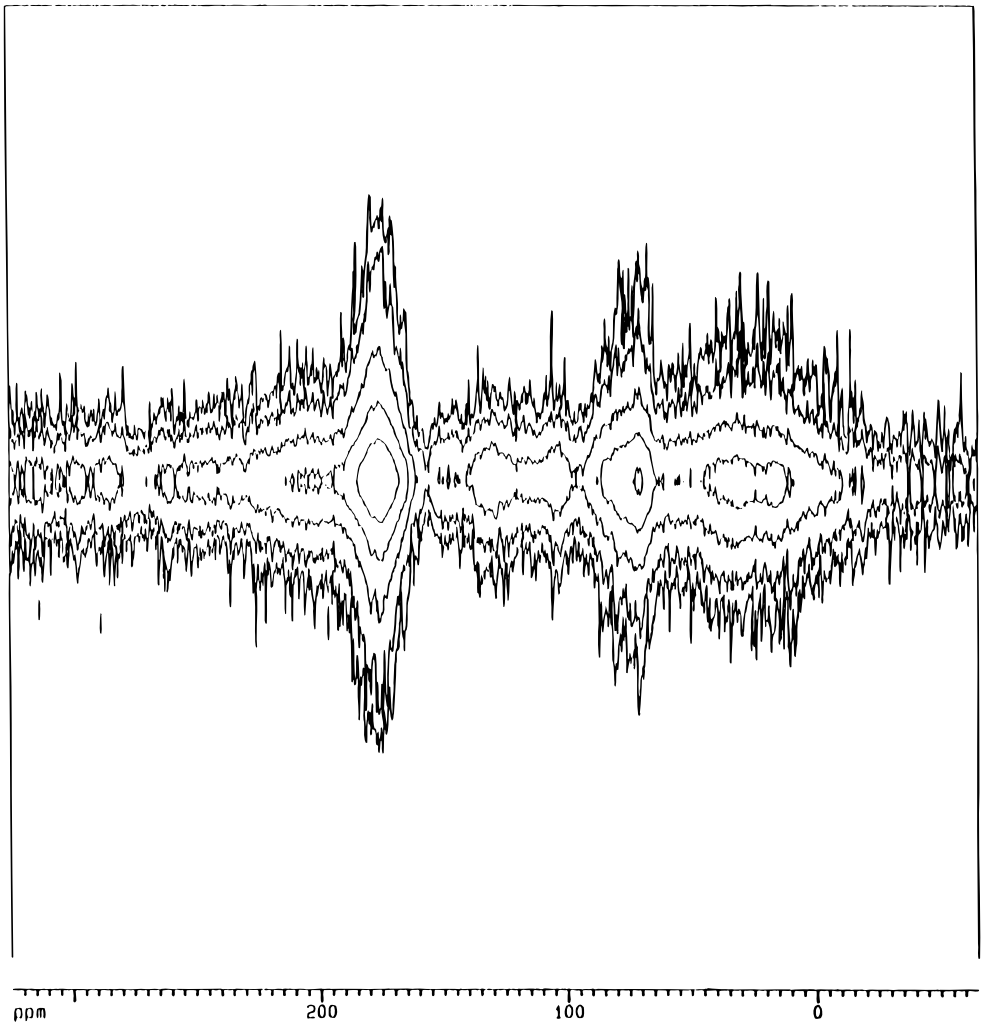

FIGURE 3. Two-dimensional dipolar dephasing spectrum of LFA. The vertical axis, which is in arbitrary units, represents dipolar dephasing, and the horizontal axis represents chemical shift; see text for details.

Intensity distribution was interpreted in terms of the following chemical shift regions (*29*): unsubstituted aliphatic carbon (0−50 ppm), carbohydrate; carbon singly bonded to O or N heteroatoms (50−96 ppm), carbon singly bonded to two O atoms (96−108 ppm), aromatic carbons (108−145 ppm), phenolic carbons (145−162 ppm), carboxyl carbons

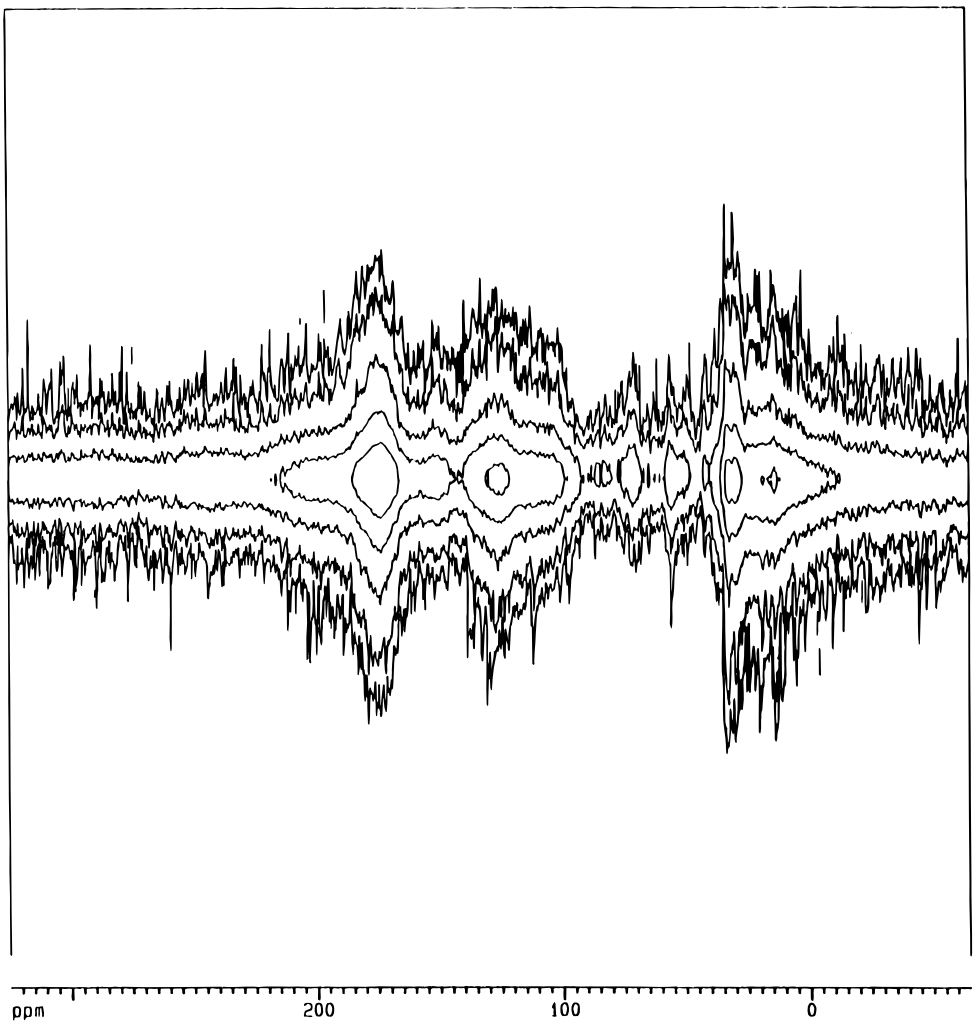

FIGURE 4. Two-dimensional dipolar dephasing spectrum of LHA. The vertical axis, which is in arbitrary units, represents dipolar dephasing, and the horizontal axis represents chemical shift: see text for details.

(162−190 ppm), and ketonic carbons (190−220 ppm). For the LHA sample, the 50−90 ppm region was subdivided into two regions: carbohydrate 1; aliphatic esters, ethers, methoxyl, and ethoxyl (50−60 ppm), and carbohydrate 2 (60−96 ppm). The uncertainties of these numbers are of the same order of magnitude as the experimental error.

Results and Discussion

Structural Importance of Various Functionalities. Consider first chemical shift evidence. Figure 2 shows the 1D chemical shift spectra of LFA and LHA. The integrated area of each region in the LFA and LHA spectra are expressed as a percentage of the total observable carbons (%TOC) in Tables 1 and 2, respectively. From these results, it can be seen that LFA is mostly aliphatic/carbohydrate, while LHA is mostly aliphatic/aromatic in terms of structural units. The fact that aliphatic units play a major role in the molecular structures of LFA is in no way unexpected, since previous fulvic acid NMR data (*5*, *30*) have shown that the aliphatic moieties of fulvic acid are of greater importance than had once been thought (*31*). The fact that aliphatic moieties also play an important role in LHA is less expected and indicates that the aliphatic moieties may deserve more attention in considering humic substances. For LFA, we emphasize the importance that the carbohydrate moieties play in structure, since it has often been assumed that aromatic moieties play the dominant functional role in humic substances.

Further evidence of structure comes from $T_2(^{13}C)$ relaxation times. These times are reported in Tables 1 and 2 for both LFA and LHA, respectively. In general, shorter relaxation times reflect reduced mobility (*15*). The $T_2(^{13}C)$ in all regions are shorter for LHA than for LFA. Thus, LHA's structural units appear to be less mobile and larger dynamic units as expected. If the $T_2(^{13}C)$ values of LFA moieties are compared, it can be seen that the aliphatic moieties are the least mobile and probably largest, while the carbohydrate and aromatic moieties are significantly smaller. For LHA, the $T_2(^{13}C)$ times suggest that the aliphatic, ester, ether, and carbohydrate moieties are the largest, while the aromatic moieties are somewhat smaller. These data once again underline that aliphatic and carbohydrate moieties play an important structural role in polymeric networks.

The spectra in Figure 2 and the %TOC data in Tables 1 and 2 show that LFA is much more functionalized that is LHA and that the carboxyl groups constitute the majority of functionalization in both LFA and LHA. Although, phenolic groups are present in both LFA and LHA, it is unlikely they are sufficiently abundant to account for all weak acid ($pK_a = 8-10$) functionality. This is particularly the case for LFA. This leads to the new conclusion that much of the weak acid functionality is located on the aliphatic/carbohydrate moieties. This is supported by the major peak in the chemical shift range between 65 and 80 ppm, which can be assigned to carbohydrate -OH. This interpretation is not contradicted

by the results of potentiometric titration (*27*). Originally weak pK_a values were assigned to phenolic groups, but hydroxyl groups located on carbohydrate moieties may be responsible.

The data in Table 1 also shows that the content of carboxylic carbons is approximately three times that of aromatic carbons. From these data it can be inferred that LFA is highly funcionalized and the majority of this functionality is not on the aromatic moieties, but on the aliphatic/carbohydrate moieties. This inference is supported by the DD spectrum of LFA, shown in Figure 3. From this spectrum, it can be seen that the CH coupling is much weaker for the aliphatic and carbohydrate moieties than it is for the aromatic moieties. The explanation for this is that the aliphatic and carbohydrate carbons are highly functionalized carrying few protons, while the aromatic moieties are not. The interpretation is further supported by the fact that the CH coupling of the carboxyl carbons is very weak, while the CH coupling of the phenolic carbons is somewhat stronger. The weakness of the carboxyl carbons CH coupling indicates few neighboring protons. The relative strength of the CH coupling of the phenols also indicates that the aromatic rings bearing the phenolic OH are protonated.

The $T_2(^{13}C)$ values for the carboxyl carbons also support the inference that the carbohydrate carbons are highly functionalized. The $T_2(^{13}C)$ values of the carboxyl carbons are seen to be most comparable to the $T_2(^{13}C)$ values of the carbohydrate carbons (Table 1). There is also evidence from the $T_2(^{13}C)$ values that the more mobile carbohydrate moieties are also the most functionalized. The $T_{1\rho}(^1H)$ values are consistent with the interpretations just given.

Turning to LHA, the data in Table 2 indicate enough aromatic carbons in LHA to support all the carboxyl groups. Thus, there is no evidence contrary to the common view that the majority of the acid functionality of humic acid is on the aromatic moieties. This finding is supported by the DD spectrum of LHA, shown in Figure 4. From this spectrum, it can be seen that the CH coupling in the aromatic domain is very weak, almost of the same order as that of the carboxyl carbons. The weakness of this CH coupling can be explained if the aromatic moieties are highly functionalized. The weakness of the phenolic CH coupling (recall the LFA phenolic CH coupling strength) supports this view. The carbohydrate/aliphatic region of the spectrum reveals strong CH coupling, indicating less substitution in these regions. The weak CH coupling in the aliphatic region of the spectrum can be explained by the methyl groups (-CH_3 groups have very weak CH couplings, due the high rate of rotation). Apparently, the aliphatic region is highly -CH_3 substituted.

The LHA $T_2(^{13}C)$ values support the interpretation. The $T_2(^{13}C)$ of the carboxyl carbons are most comparable to the $T_2(^{13}C)$ of the aromatic carbons (Table 2). Again, it appears that the aromatic rings are highly functionalized.

The $T_{1\rho}(^1H)$ values of LHA are shorter than those of LFA for the carboxyl, phenolic, and aromatic carbons by about 1.5 ms (or 28%). A shorter $T_{1\rho}(^1H)$ can come about by three mechanisms: molecular motion, a paramagnetic impurity, or the presence of radicals. The first mechanism is very unlikely since the aromatic moieties are the least likely to be affected by motional effects because of ring rigidity. A paramagnetic impurity (e.g., Fe (III)) is possible but because of the method by which this sample was purified rather unlikely. This leads to the conclusion that the reduction in $T_{1\rho}(^1H)$ of the carboxyl, phenolic, and aromatic moieties of LHA, in comparison to LFA, is due to stable organic radicals on the aromatic moieties. This conclusion is also supported by the poorer signal to noise ratio for LHA in comparison to LFA even though the same amount of material was loaded into the rotor. This is consistent with ESR results on similar humics (*32*), and again implies that aromatic ring functionalities allow for stable radicals.

Structural Implications. This study leads to the following structural implications for LFA and LHA.

LFA. A structural model for LFA emerges in which there appears to be three major components. These are a group of large relatively immobile structural units, some mobile unfunctionalized units, and some highly substituted functionalized units. The large relatively immobile units are mainly aliphatic and unfunctionalized. The unfunctionalized mobile units are mainly aromatic, while the functionalized mobile units are mainly carbohydrate in nature. The mobile carbohydrate units have both hydroxyl and carboxyl functionality. This structural model raises an important question as to the relative importance of functionality on carbohydrate moieties and aromatic moieties in metal binding.

LHA. The structural model for LHA that emerges consists of one type of major immobile unit associated with slightly more mobile units that are mainly aromatic in nature. These slightly smaller and more mobile units are highly substituted and are expected to be the major players in metal and acidic proton binding.

In conclusion, the models suggest significantly different composition for LFA and LHA. The LFA structural model is less like previously proposed structural models for fulvic acid. The LHA structural model is evolved from earlier proposed structural models for humic acid and is consistent with some of the more recent structural proposels, such as the Donan gel model put forward by Benedetti et al. (*33*). It is especially important that all results emphasize the mixture of different size fragments in humic materials. Thus, no effort is made to show a "typical structural formula" as has often been done, and we believe such structures can be highly misleading. Dynamic models are needed.

Acknowledgments

We acknowledge the Natural Science and Engineering Research Council of Canada and the University of Calgary for financial support. We would also like to thank Dr. E. O. Stejskal for many enlightening discussions and Drs. D. E. Axelson, C. M. Preston, S. O. Smith, and R. Yamdagni for many useful discusions. We cordially thank Mrs. Qiao Wu and Dr. R. Yamdagni for technical assistance.

Literature Cited

(1) Cook, R. L.; Langford, C. H.; Yamdagni, R.; Preston, C. M. *Anal. Chem*. **1996**, *68*, 3979−3986.
(2) Cook, R. L. Manuscript submitted.
(3) Cook, R. L.; Langford, C. H. *Anal. Chem*. **1995**, *67*, 174−180.
(4) Preston, C. M. *Soil Sci.* **1996**, *161*, 144−167.
(5) Wilson, M. A. *NMR Techniques and Applications in Geochemistry and Soil Chemistry*; Pergamon Press: Oxford, 1987.
(6) Fründ, R.; Lüdemann, H.-D. *Sci. Total Environ.* **1989**, *81/82*, 157−168.
(7) Kinchesh, P.; Powlson, D. S.; Randall, E. W. *Eur. J. Soil. Sci.* **1995**, *46*, 125−138.
(8) Wershaw, R. L., Mikita, M. A., Eds. *NMR of humic substances and coal. Techniques, problems and solutions*; Lewis Publishers: Chelsea, MI, 1987.
(9) Jurkiewicz, A.; Marciel, G. E. *Anal. Chem*. **1995**, *67*, 2188−2194.
(10) Pan, V. H.; Maciel, G. E. *Fuel* **1993**, *72*, 451−468.
(11) Snape, C. E.; Axelson, D. E.; Botto, R. E.; Delpeich, J. J.; Tekely, P.; Gerstien, B. C.; Pruski, M.; Maciel, G. E.; Wilson, M. A. *Fuel* **1989**, *68*, 547−560.
(12) Schnitzer, M.; Preston, C. M. *Soil Sci. Soc. Am. J.* **1986**, *50*, 326−331.
(13) Metz, G.; Wu, X.; Smith, S. O. *J. Magn. Reson. Ser. A* **1994**, *10*, 219−227.
(14) Voelkel, R. *Angew. Chem. Int. Ed. Engl.* **1988**, *27*, 1468−1483.
(15) Axelson, D. E. *Solid State Nuclear Magnetic Resonance of Fossil Fuels*; Multiscience Publications Ltd., Canadian Government Publishing Centre, Supply and Services Canada: 1985; Chapters 1−3 and 6.
(16) Stejskal, E. O.; Memory, J. D. *High Resolution NMR in the Solid State: Fundamentals of CP/MAS*; Oxford University Press: New York, 1994; Chapters 2 and 3.

(17) Earl, W. L.; VanderHart, D. L. *Macromolecules* **1979**, *12*, 762−767.
(18) Ernst, R. R.; Bodenhausen, G.; Wokaun, A. *Principles of Nuclear Magnetic Resonance in One and Two Dimensions*; Oxford University Press: Oxford, 1994; Chapter 6.
(19) Freeman, R. A. *Handbook of Nuclear Magnetic Resonance*; Longman Scientific & Technical: New York, 1988; pp 291−297.
(20) Opella, S. J.; Frey, M. H. *J. Am. Chem. Soc.* **1974**, *101*, 5854−5856.
(21) Wilson, M. A. *J. Soil Sci.* **1984**, *35*, 209−215.
(22) Griffith, S. M.; Schnitzer, M. *Soil Soc.* **1975**, *120*, 126−131.
(23) Schnitzer, M.; Skinner, S. I. M. *Soil Soc.* **1968**, *105*, 392−396.
(24) Bruccoleri, A.: Pant, B. C.; Sharma, D. K.; Langford, C. H. *Environ. Sci. Technol.* **1993**, *27*, 889−894.
(25) Wang, Z. D.; Pant, B. C.; Langford, C. H. *Anal. Chim. Acta* **1990**, *232*, 43−49.
(26) Wang, Z. D.; Gamble, D. S.; Langford, C. H. *Environ. Sci. Technol.* **1992**, *26*, 560−565.
(27) Wang, Z. D. Ph.D. Thesis, Concordia University, Montreal, 1989.
(28) Schnitzer, M.; Preston, C. M. *Soil Sci. Soc. Am. J.* **1986**, *50*, 326−331.
(29) Malcolm, R. L. *Anal. Chim. Acta* **1990**, *232*, 19−30.
(30) Hatcher, P. G.; Schnitzer, M.; Dennis, L. W.; Maciel, G. E. *Soil Sci. Soc. Am. J.* **1981**, *45*, 1089−1094.
(31) Stevenson, F. J. *Humus Chemistry: Genesis, Composition, Reactions*, 2nd ed.; John Wiley & Sons, Inc.: New York, 1994; Chapter 12.
(32) Senesi, N.; Schnitzer, M. In *Environmental Biogeochemistry and Geomicrobiology*; Krumbein, E. W., Ed.; Ann Arbor Science: Ann Arbor, MI, 1978; pp 467−481.
(33) Benedetti, M. F.; Van Riemsdijk, W. H.; Koopal, L. K. *Environ. Sci. Technol.* **1996**, *30*, 1805−1813.

Received for review June 3, 1997. Revised manuscript received October 30, 1997. Accepted November 1, 1997.

ES970488C